

Effect of transmit array phase relationship on local Specific Absorption Rate (SAR)

L. M. Angelone^{1,2}, N. Makris³, C. Vasios¹, L. Wald¹, G. Bonmassar¹

¹A. Martins Center for Biomedical Imaging, Massachusetts General Hospital, Charlestown, MA, ²Biomedical Engineering Department, Tufts University, Medford, MA, ³Center for Morphometric Analysis, Massachusetts General Hospital, Charlestown, MA
angelone@nmr.mgh.harvard.edu, http://www.nmr.mgh.harvard.edu/~angelone

ABSTRACT

We studied the range of local and average Specific Absorption Rate (SAR) values [1] possible when the phase relationship between individual transmit elements in a transmit array is altered. The B_1 and E_1 RF fields were modeled for 8 channel array of circular loop elements using the FDTD algorithm. An anatomically accurate high resolution (1mm³) head model with 29 tissue types was used.

There was a 3-fold difference for SAR averaged in specific tissues (CSF and eyes) for linear vs. circular excitation. There was a 5-fold change between minimum and maximum slice-averaged SAR for generic phase configuration. An extensive study on the entire high-resolution head model with a higher number of phase configurations is suggested.

1. NUMERICAL MODEL

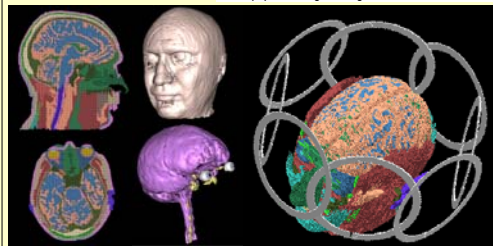
• **A high-resolution (1mm³ isotropic) head model based on the anatomical MRI data of an adult male subject [2]**

TISSUE	Density (kg/m ³)	Weight (g)	300 MHz σ (S/m)	ϵ_r
CSF	1010	2035	2.22	72.73
Grey Matter	1040	512.82	0.69	60.02
White Matter	1040	916.70	0.41	43.77
Adipose	920	36.45	0.08	11.74
Air	1	0.09	0.00	1.00
Bone Cortical	1850	316.15	0.08	23.16
Aqueous-Humor	1000	0.16	1.00	100.00
Conn.Tissue ^{**} (arterial and venous)	1036	31.44	0.63	46.66
Cornea	1000	0.07	1.15	61.37
CSF_SA	1010	17.41	2.22	72.73
Diploe	970	133.00	0.17	12.13
Dura	1850	381.01	0.80	47.96
Ear	1100	44.31	0.55	46.77
Epididymis	1010	389.67	0.63	52.00
Inner-Tablet	1850	477.94	0.22	23.16
Lens ^{**} (crystallin)	1100	0.46	0.55	46.77
Muscle	1040	1133.83	0.69	59.97
Nasal-Structures	1100	61.24	0.55	46.77
Nerve	1040	6.37	0.42	36.91
Ombra-Fat	920	38.77	0.08	11.74
Outer-Tablet	1850	121.57	0.22	23.16
Subcutaneous Tissue ^{**} (cuticle and blood)	1036	47.02	0.63	42.23
RCS	1170	6.34	0.58	58.50
SC-Fat/Muscle ^{**} (fat and muscle)	980	374.52	0.38	35.36
Soft-Tissue ^{**} (muscle, skin, tendon, bone, fat)	1226.5	194.11	0.40	36.63
Signal-Cord	1040	7.20	0.42	36.91
Tooth	1850	39.27	0.22	23.16
Tongue	1040	19.74	0.74	59.00
Vitreous-Humour	1000	8.26	1.51	69.00

Tissue properties as in [3] excluding ** Tissue properties as weighted average

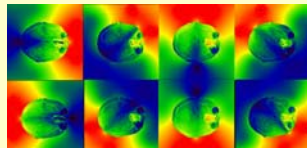
• **29-tissues manually segmented**

• **Eight RF coils centered around the head model driven with 1A current source.**

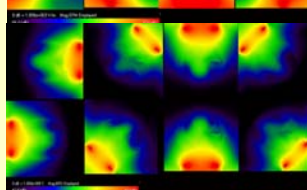


2. SINGLE SURFACE COIL EFFECT OF POSITION ON EM FIELD

Steady State E field (top) and B field (bottom) distribution computed for each coil individually.



The EM distribution depends on the coil position and on the head model shape [3].



3. SINGLE SURFACE COIL EFFECT OF POSITION ON SAR

• **34-fold change of averaged SAR in the eyes (coil 1 vs. coil4).**

SAR (W / kg)	COIL 1	COIL 2	COIL 3	COIL 4	COIL 5	COIL 6	COIL 7
1W Input Power Max for 1mm ³							
Whole - head	16.73	0.32	5.05	0.13	9.18	0.35	2.72
Grey Matter	3.99	0.50	1.39	0.22	3.15	0.61	1.55
Diploe	2.32	0.18	1.49	0.07	2.92	0.23	1.43
Epidermis	9.97	0.51	4.81	0.23	7.77	0.55	2.71
Vitreous-Humour	2.54	1.04	1.57	0.44	1.13	0.41	0.08

4. SINGLE SURFACE COIL COMBINED EFFECT OF POSITION AND PHASE

SAR is defined as [4]:

$$SAR = \frac{\sigma}{2\rho} \langle |E(\vec{r}, t)|^2 \rangle$$

The electric field in each voxel r at the time t_0 will be given by the superposition of E field for each of the N coils:

$$|\vec{E}(\vec{r}, t)|^2 = \left| \sum_{n=1}^N \vec{E}(\vec{r}, t) \right|^2 = \left| \sum_{n=1}^N E_{n,x}(\vec{r}, t) \hat{x} + \sum_{n=1}^N E_{n,y}(\vec{r}, t) \hat{y} + \sum_{n=1}^N E_{n,z}(\vec{r}, t) \hat{z} \right|^2$$

For a sinusoidal source the value of the x component of the electric field for each point r will be obtained as (similarly for y and z direction):

$$\sum_{n=1}^N |E_{n,x}(\vec{r}) \sin(\omega t + \varphi_{n,x}(\varphi_n, \vec{r}))| = \sum_{n=1}^N |E_{n,x,0}(\vec{r}) \sin(\omega t + \varphi_{n,x}(\varphi_n, \vec{r}))| \cos(\varphi_{n,x}(\varphi_n, \vec{r}) - \varphi_m(\varphi_m, \vec{r}))$$

Corresponding SAR distribution will be:

$$SAR_x = \iiint_V \left(\frac{\sigma(\vec{r})}{2\rho(\vec{r})} \left[\frac{1}{2} \sum_{n=1}^N |E_{n,x,0}(\vec{r})|^2 + \frac{1}{T} \sum_{n=1}^N \sum_{m=1}^N |E_{n,x,0}(\vec{r})| |E_{m,x,0}(\vec{r})| \cos(\varphi_{n,x}(\varphi_n, \vec{r}) - \varphi_m(\varphi_m, \vec{r})) \right] \right) d\vec{r}$$

That implies:

$$\frac{\partial}{\partial \varphi_n} \left\{ \iiint_V \left(\frac{\sigma(\vec{r})}{2\rho(\vec{r})} \left[\frac{1}{2} \sum_{n=1}^N |E_{n,x,0}(\vec{r})|^2 + \frac{1}{T} \sum_{m=1}^N |E_{n,x,0}(\vec{r})| |E_{m,x,0}(\vec{r})| \cos(\varphi_{n,x}(\varphi_n, \vec{r}) - \varphi_m(\varphi_m, \vec{r})) \right] \right) d\vec{r} \right\} = 0$$

that is equivalent to:

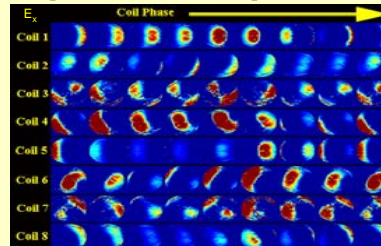
$$\iiint_V \sum_{n=1}^{N-1} \sum_{m=n+1}^N |E_{n,x,0}(\vec{r})| |E_{m,x,0}(\vec{r})| \left[\sin(\varphi_{n,x}(\varphi_n, \vec{r}) - \varphi_m(\varphi_m, \vec{r})) \frac{\partial \varphi_m}{\partial \varphi_n} \right] d\vec{r} = 0 \quad \text{for } i = n$$

$$\iiint_V \sum_{n=1}^{N-1} \sum_{m=n+1}^N |E_{n,x,0}(\vec{r})| |E_{m,x,0}(\vec{r})| \left[\sin(\varphi_{n,x}(\varphi_n, \vec{r}) - \varphi_m(\varphi_m, \vec{r})) \frac{\partial \varphi_n}{\partial \varphi_m} \right] d\vec{r} = 0 \quad \text{for } i = m$$

➤ SAR function of each

$$\sin(\varphi_{n,x}(\varphi_n, \vec{r}) - \varphi_m(\varphi_m, \vec{r}))$$

➤ An accurate modeling of the phase delay for each point r , coil n and coil phase φ_n is required



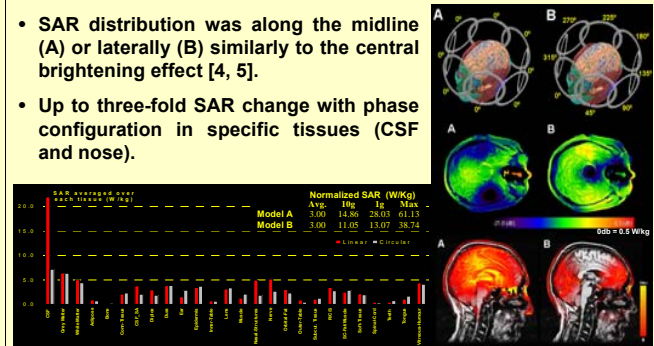
ACKNOWLEDGEMENTS. We thank G. Wiggins, V. Alagappan, H. Millan, S. Alfhors (A. Martins Center), as well as F. Schmitt, F. Hebrank, A. Potthast, and G. Brinker (Siemens Medical) for the useful discussions during this study. Work supported by NIH grants R01 EB002459, P41 RR014075, and the MIND institute.

REFERENCES. [1]. I.E.C. 601-2-33; [2] Angelone et al. Proc. ISMRM 2005; [3] Gabriel et al, 1996; [3] Chou et al. Bioelectromagnetics 1996. [4] Ibrahim, T.S., et al., IEEE Trans Biomed Eng, 2005. 52(7): p. 1278-84. [5] Collins, C.M., et al., J Magn Reson Imaging, 2003. 18(3): p. 383-8. [6] Van der Berg ISMRM proc. 2005.

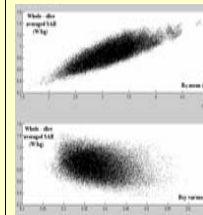
Linear (A) vs. circular (B) excitation Local and whole-head SAR distribution

• SAR distribution was along the midline (A) or laterally (B) similarly to the central brightening effect [4, 5].

• Up to three-fold SAR change with phase configuration in specific tissues (CSF and nose).

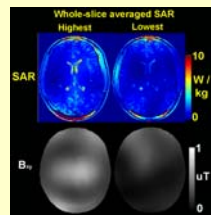


Random phase excitation: slice - averaged SAR and B₁ field

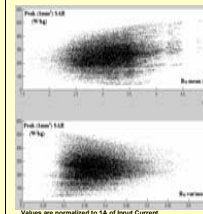


• Low/high averaged SAR corresponded to low/high B_{xy} mean values [6].

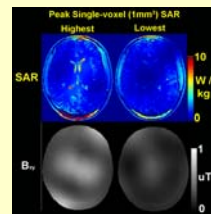
• Non-linear distribution for SAR vs. normalized variance B_{xy}



(1mm³) peak SAR and B₁ field



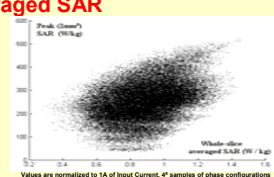
• Non-linear distribution for both peak SAR vs B_{xy} mean and peak SAR vs normalized B_{xy} variance



Peak SAR vs. Averaged SAR

➤ Max. / Min. slice - averaged SAR = 5

➤ Max. / Min. peak (1mm³) SAR = 10



CONCLUSIONS

➤ Transmit array's phase relationship can affect averaged and peak SAR values, as well as B_1 distribution.

➤ Max. / Min. slice - averaged SAR for a generic phase configuration = 5

➤ An extensive study on the entire high-resolution head model with a higher number of phase configurations is strongly suggested.